Simulation of industrial catalytic-distillation process for production of methyl *tert*-butyl ether by developing user's model on Aspen plus platform

Jie Bao [a,*], Buliang Gao [b], Xiaoqun Wu [c], Makoto Yoshimoto [a], Katsumi Nakao [a]

[a] *Department of Applied Chemistry and Chemical Engineering, Faculty of Engineering, Yamaguchi University, Tokiwadai 2-16-1, Ube, Yamaguchi 755-8611, Japan*
[b] *Qilu Petrochemical Research Institute of Sinopec, Zibo, Shandong 255400, China*
[c] *Department of Chemical Engineering, Zhejiang University, Hangzhou, Zhejiang 310071, China*

Abstract

The industrial catalytic-distillation process for the production of methyl *tert*-butyl ether (MTBE) from methanol and isobutylene was simulated by developing the process model as a user modular on Aspen plus platform. The model utilizes the Aspen plus system and retains the characteristics of the self-designed model, which has been verified in various scale-up processes. The experimentally determined reaction kinetics was applied in the model. NRTL and Redlick–Kwong–Soave equations were selected for the vapor–liquid equilibrium calculation. The NRTL binary interaction parameters were estimated from the experimental data of the two-component vapor–liquid equilibrium. Two typical industrial plants for the MTBE production, one using the loose-stack-type package technology and the other using the bale-type package technology in the catalytic-distillation column, were chosen as the sample processes to demonstrate the validity of the model. The flowsheet simulations of the two industrial plants were done on Aspen plus platform, in which the simulation of the catalytic-distillation column used the developed user modular. The results show that fair agreements between the calculated and operating data were obtained.
© 2002 Elsevier Science B.V. All rights reserved.

1. Introduction

Catalytic-distillation technology for the production of methyl *tert*-butyl ether (MTBE) has been commercialized to the scale of annual productivity more than 100,000 t in many countries [1–4]. To meet the needs of the design for the new plants and optimization of the existing ones, an accurate mathematical model for simulating the industrial-scale catalytic-distillation process is needed. On the other hand, very few industrial cases were reported, although many studies were devoted to the modeling of catalytic-distillation process [5]. A practical model should have at least the following capacities: (1) it describes the structural characteristics of catalyst packages used in industrial processes, (2) the fundamental parameters such

as reaction kinetics and vapor–liquid equilibrium data are supported by either experimental data or reliable database, (3) it is verified by industrial operation data, and (4) the industrial flowsheet can be simulated, not merely in a single catalytic-distillation unit.

In our previous reports, the model for the catalytic-distillation process in the MTBE production was successfully applied in various scales from bench tests, pilot tests, and in a semi-industrial plant with the annual productivity of 2000 t MTBE [3,6]. With the rapid industrialization rate of the process, some shortages in the model appeared. First, the model was a self-designed Fortran program used to simulate a single catalytic-distillation unit. Thus, the whole flowsheet composed of different unit operations could not be simulated. Second, only five components were used in the model instead of the 12 main components in the real case. The eight main hydrocarbon components were represented by only three key components, isobutylene, 1-butane and 1-butylene. This certainly created the inaccuracy in the real industrial operation with massive productivity. Third, the database and calculation functions in the previous model

* Corresponding author. Present address: Department of Bioscience and Biotechnology, Faculty of Engineering, Okayama University, Tsushimanaka 3-1-1, Okayama 700-8530, Japan. Tel.: +81-86-251-8202; fax: +81-86-231-0257.
E-mail address: baojie@biotech.okayama-u.ac.jp (J. Bao).

Nomenclature

A, B, C, D	coefficients of tridiagonal matrix
A_1	Arrhenius frequency factor of rate constant k_1
A_2	Arrhenius frequency factor of rate constant k_2
b	NRTL binary interaction parameter
c	component number
C	molar concentration (mol/m^3)
E_1	activation energy of rate constant k_1 (J/mol)
E_2	activation energy of rate constant k_2 (J/mol)
FI1	molar flowrate of the mixed C4/methanol feedstock (mol/s)
FI2	molar flowrate of the methanol feedstock (mol/s)
h	enthalpy of liquid stream (J/mol)
H	enthalpy of vapor stream (J/mol)
ΔH	heat of reaction (J/mol)
HI	enthalpy of feedstock (J/mol)
k_1	first-order rate constant of the forward reaction of reaction (1) (s^{-1})
k_2	first-order rate constant of the reverse reaction for reaction (1) (s^{-1})
L	liquid molar flowrate (mol/s)
N	number of equilibrium stages
NC1	start stage of catalyst packing
NC2	end stage of catalyst packing
NF1	stage of the mixed C4/methanol feedstock
NF2	stage of the methanol feedstock
P	pressure of the system (MPa)
P^0	vapor Antoine pressure (MPa)
ΔQ	total heat of reaction (J)
r	reaction rate (mol/m^3 s)
R	gas constant (J/mol K)
ΔR	reacted moles of components (mol)
t	time (s)
T	temperature (K)
v	molar volume (m^3)
V	vapor molar flowrate (mol/s)
V_C	catalyst volume (m^3)
V_L	liquid volumetric flowrate (m^3/s)
V_T	catalyst space velocity (s^{-1})
x	molar fraction of liquid
X_B	conversion of isobutylene
y	molar fraction of vapor
ZI	molar fraction of feedstock

Greek letters

α	NRTL binary interaction parameters
α, δ	empirical coefficients of catalyst package
γ	liquid activity coefficient
ρ	liquid molar density (mol/m^3)
ϕ	vapor fugacity

Subscripts

B	isobutylene
i	component ($1 \leq i \leq c$)
j	equilibrium stage ($1 \leq j \leq N$)
M	methyl *tert*-butyl ether

Superscripts

k	reaction section in the small reactor at each stage ($1 \leq k \leq$ KS)
KS	number of package layers at each stage

were limited and it was difficult to carry out the detailed optimization calculations.

Aspen plus system is one of the standard software for flowsheet simulation in the processing industries. It is supported by strong databases, complete sets of modules, and flexible simulation tools. The system provides many built-in modules for simulating various processes, and the modular for simulating the reactive-distillation process is also one of them. An important assumption is given in this reactive-distillation modular, that is, both reaction and separation are assumed to take place in the liquid phase in the column trays or packings. Therefore, the liquid residue time or liquid holdup is required [7,8]. In the heterogeneous catalytic-distillation process, however, the solid catalyst particles are packed into many catalyst envelopes, instead of the homogeneous dispersion in the liquid phase in the trays or packings. The reactions occur inside the catalyst packages when the liquid contacts the catalyst particles. Then, the products flow out of the packages, and the separation takes place on the trays or packings through the count-current vapor–liquid contact. This fact indicates a major difference between homogeneous and heterogeneous processes: the reaction and separation actually take place in the different locations of the column in the heterogeneous process, i.e. reaction in the catalyst packages and separation in the trays or packings. Therefore, the parameters of liquid residue time or the liquid holdup on the trays or packings in the heterogeneous process can only be used in the separation calculation, whereas the reaction calculation needs the parameters of contacting time of liquid with catalyst in the catalyst packages. Hence, we may conclude that the built-in reactive-distillation modular in Aspen system is not suitable for simulating the heterogeneous catalytic-distillation process for the above reason.

To overcome the above problems, an effort was made in this study to develop a self-defined model for simulating heterogeneous catalytic-distillation, and then to connect the model with Aspen plus as a user modular. In the new model,

the contacting time of liquid with catalyst is represented by the catalyst space velocity V_T appearing in the reaction equations. In this way, not only the user modular takes advantages of strong database, flexible simulation functions and optimization tools of Aspen plus system, but it also keeps the characteristics of the model that had been verified in the previous scale-up experiments.

The purpose of this study is (1) to establish a mathematical model oriented to the heterogeneous catalytic-distillation structure, (2) to build the mathematical model in the user modular provided by Aspen plus and compile it into an available modular on Aspen plus platform, (3) to connect the database and calculation functions of Aspen plus with the user model, and (4) to apply the model into the industrial applications.

2. Reaction kinetics and thermodynamics

2.1. Reaction kinetics

The synthesis of MTBE from methanol and isobutylene catalyzed by Amberlyst-15 or similar sulphonic ion-exchange resin catalysts [3] is a reversible etherification as shown in Eq. (1):

$$CH_3C(CH_3)=CH_2 \text{ (B)} + CH_3OH \underset{k_2}{\overset{k_1}{\rightleftharpoons}} CH_3C(CH_3)_2OCH_3 \text{ (M)} \quad (1)$$
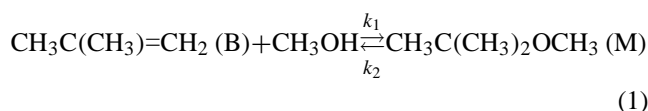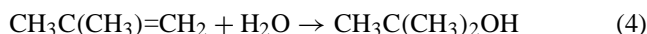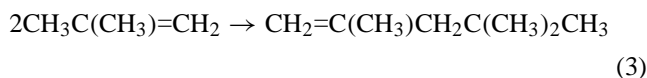
According to Yang et al. [9], the forward reaction of reaction (1) is first-order with respect to the isobutylene concentration and zero-order with respect to the methanol concentration, respectively, and the reverse reaction is first-order with respect to the MTBE concentration as shown in Eq. (2):

$$-r_B = k_1 C_B - k_2 C_M \quad (2)$$

where $k_1 = A_1 \exp(-E_1/RT)$ and $k_2 = A_2 \exp(-E_2/RT)$ are the first-order rate constants for the forward and reverse reactions, respectively. The values of Arrhenius frequency factors A_1, A_2 and activation energy E_1, E_2 for the sulphonic ion-exchange resin catalyzed reaction are listed in Table 1 [9]. The reaction kinetic data had been verified in several industrial applications of the MTBE production, in which the fixed-bed reactor packing of the same catalyst was used.

The main side reactions are the dimerization of isobutylene to diisobutylene (2,4,4-trimethyl-1-pentene), and the hydration of isobutylene to *tert*-butyl-alcohol (TBA) as

Table 1
Arrhenius parameters of rate constant k_1 and k_2 for MTBE synthesis catalyzed by sulphonic ion-exchange acidic resin catalysts

A_1	A_2	E_1 (J/mol)	E_2 (J/mol)
6.50×10^5	1.36×10^8	4.74×10^4	7.04×10^4

shown in Eqs. (3) and (4), respectively:

$$2CH_3C(CH_3)=CH_2 \rightarrow CH_2=C(CH_3)CH_2C(CH_3)_2CH_3 \quad (3)$$

$$CH_3C(CH_3)=CH_2 + H_2O \rightarrow CH_3C(CH_3)_2OH \quad (4)$$

The kinetic study shows that reaction (3) can only take place when the addition of methanol is insufficient (the molar ratio of methanol to isobutylene is lower than 0.8) [9]. Since the methanol addition is carefully arranged to allow the molar ratio of methanol to isobutylene to be higher than 0.8 at each stage of the catalytic-distillation column, reaction (3) can be reasonably neglected in the catalytic-distillation unit. For reaction (4), the minor water in hydrocarbon and methanol feedstocks is consumed in the pre-reactor before it is fed into the catalytic-distillation column. Therefore, reaction (4) can also be neglected in the catalytic-distillation unit. The products of the two side reactions are considered in the vapor–liquid equilibrium calculation, whereas the reaction kinetics are not included in the calculation.

2.2. Vapor–liquid equilibrium

A typical industrial process for the MTBE production involves at least 12 components: propylene, isobutane, 1-butane, 1-butylene, isobutylene, *cis*-2-butylene, *trans*-2-butylene, methanol, MTBE, diisobutylene, TBA, and water. Since methanol associates almost all hydrocarbon components into azeotropic pairs, the system shows the strong non-ideal properties. The vapor–liquid equilibrium constant K_i for component i is expressed in Eq. (5):

$$K_i = \gamma_i \frac{\phi_i^0}{\phi_i} \frac{P_i^0}{P} \exp\left[\frac{v_i(P - P_i^0)}{RT} \right] \quad (5)$$

where γ_i is the liquid activity coefficient, ϕ_i^0 and ϕ_i the vapor fugacity in pure and mixture state, respectively, P_i^0 the vapor Antoine pressure, v_i the molar volume and P is the total pressure of the system. The NRTL equation and Redlick–Kwong–Soave equation are selected to calculate liquid activity coefficient γ_i and the vapor fugacity ϕ_i (and ϕ_i^0), respectively. The NRTL activity coefficient equation is expressed in Eq. (6):

$$\ln \gamma_i = \frac{\sum_j x_j \tau_{ji} G_{ji}}{\sum_k x_k G_{ki}} + \sum_j \frac{x_j G_{ij}}{\sum_k x_k G_{kj}} \left(\tau_{ij} - \frac{\sum_m x_m \tau_{mj} G_{mj}}{\sum_k x_k G_{kj}} \right) \quad (6)$$

where $G_{ij} = \exp(-\alpha_{ij}\tau_{ij})$, $\tau_{ij} = b_{ij}/T$ and $\alpha_{ij} = \alpha_{ji}$. The NRTL binary interaction parameters b_{ij}, b_{ji} and α_{ij} were estimated from the experimental data of two-component vapor–liquid equilibrium using data regression system (DRS) in the Aspen plus system, followed by the thermodynamics consistence check. The estimated NRTL binary

Table 2
Values of NRTL binary interaction parameters for components involved in MTBE synthesis

Components i–j	b_{ij}	b_{ji}	α_{ij}
Propylene–methanol[b]	617.96	258.78	0.30
Propylene–MTBE[b]	204.97	−114.11	0.30
Propylene–tert-butyl alcohol[b]	617.96	258.78	0.30
Isobutane–methanol[a]	663.40	505.94	0.47
Isobutane–MTBE[a]	204.96	−114.11	0.30
Isobutane–tert-butyl alcohol[a]	663.40	505.94	0.47
1-Butane–methanol[a]	672.37	516.54	0.47
1-Butane–MTBE[a]	230.71	−117.97	0.47
1-Butane–tert-butyl alcohol[a]	672.37	516.54	0.47
1-Butylene–methanol[a]	695.79	440.17	0.47
1-Butylene–MTBE[a]	−288.49	440.51	0.30
1-Butylene–tert-butyl alcohol[a]	695.79	440.17	0.47
Isobutylene–methanol[a]	790.53	435.53	0.47
Isobutylene–MTBE[a]	−141.72	225.70	0.30
Isobutylene–tert-butyl alcohol[a]	790.53	435.53	0.47
Trans-2-butylene–methanol[a]	695.79	440.17	0.47
Trans-2-butylene–MTBE[a]	−288.49	440.51	0.30
Trans-2-butylene–tert-butyl alcohol[a]	695.79	440.17	0.47
Cis-2-butylene–methanol[a]	190.02	237.43	0.30
Cis-2-butylene–MTBE[a]	440.17	695.79	0.47
Cis-2-butylene–tert-butyl alcohol[a]	−162.17	46.98	0.30
Methanol–MTBE[a]	663.40	505.94	0.47
Methanol–diisobutylene[b]	204.96	−114.11	0.30
Methanol–tert-butyl alcohol[b]	663.40	505.94	0.47
Methanol–water[b]	828.39	−1329.54	0.30
MTBE–diisobutylene[b]	440.51	−288.49	0.30
MTBE–tert-butyl alcohol[b]	489.67	−240.51	0.30
MTBE–water[b]	682.05	1108.82	0.30
Diisobutylene–tert-butyl alcohol[b]	695.79	440.17	0.47
Tert-butyl alcohol–water[b]	217.51	−1395.02	0.30

[a] Parameters estimated from experimental VLE data.
[b] Parameters from Aspen database DIPPR [8].

interaction parameters b_{ij}, b_{ji} and α_{ij} are shown in Table 2. The other fundamental properties such as molar volume, heat capacity, vapor capacity and density, etc. were called from DIPPR database in the Aspen plus system.

3. Model development on Aspen plus platform

3.1. Model configuration of catalytic-distillation column

For developing a practical catalytic-distillation process, the design of an efficient catalyst package poses considerable challenges [5]. For the MTBE production process, the fine sulphonic ion-exchange resin particles with its size less than 1.0 mm have to be enveloped in various conceivable shapes [5,10–12]. Among them, two typical structures had been applied to an industrial scale of more than 100,000 t annually, one being the bale-type package [13–16] and the other the loose-stack package [6,3,17].

Two considerations are taken as the most important factors for the catalyst packages: one being the contact efficiency of liquid with catalyst, and the other being the reaction efficiency of catalyst. Correspondingly, the model

development should reflect the characteristics of the catalyst packages. Two empirical coefficients α and δ were introduced in the model: α represents the ratio of the liquid flowrate entering the catalyst package to the total liquid flowrate, reflecting the contact efficiency of liquid to catalyst (liquid flows into the passby ways in many kinds of packages). δ represents the ratio of the real reaction rate to the kinetic reaction rate under the same conditions (liquid floods through catalyst in non-plug flow in many packages). The value of α was determined by measuring the cross-area occupied by catalyst to the total cross-area in the reactive section. The value of δ was determined separately in a specially designed small reactor. The detailed procedure: put a single catalyst package in the small reactor under the same reaction and hydrodynamic conditions (same count-current vapor–liquid flowrates), then determine its reaction rate and compare with the kinetic rate. The two coefficients were used to model various types of catalyst packages during the process development from bench tests, and different scales of pilot tests [3,6]. The value of α was between 0.5 and 1.0, the value of δ was between 0.6 and 1.0.

On the other hand, the catalyst package had shown continuous improvement in both the aspects. In the final type used in the commercial plant, the design of the loose-stack package let all the liquid enter the catalyst envelope, and then flood smoothly through the catalyst container. As the result, α was 1.0 by its definition. The experimental determination of δ was also close to the unity value of 1.0, because of the perfect contacting of liquid with catalyst in the packages, and because the flow is close to the plug-flow pattern inside the packages. The trial-and-error method was used to search the most suitable value of α and δ for the bale-type package [3,6,17]. We found that the calculation results gave the best fitness to the operating ones using the unity value of 1.0 to both of the parameters. This fact indicates that the industrial packages of the bale-type package are also under the conditions of perfect contacting of liquid with catalyst and stable plug flow inside the packages. In other words, the two coefficients in the current model for the industrial simulations can be ignored. This is why we keep the coefficients in the model for consistency with the previous model [3,6], and to give them the value of 1.0 in the current industrial cases.

The equilibrium stage model based on the bale-type and loose-stack-type packages in the reactive section is shown in Fig. 1. Fig. 1(a) indicates the whole catalytic-distillation column, and Fig. 1(b) indicates the detailed structure of a typical equilibrium stage in the reactive section. There are N equilibrium stages in the column. The catalyst packages are installed from stages NC1 to NC2, forming the reactive section. The catalyst packages at each stage of the reactive section are represented by a corresponding small reactor. This small reactor is divided into several layers from 1 to KS corresponding to the real arrangement of the catalyst packages. The mixed C4 stream FI1 and pure methanol stream FI2 are fed into the column at stages NF1 and NF2, respectively. The radial gradients of composition and heat
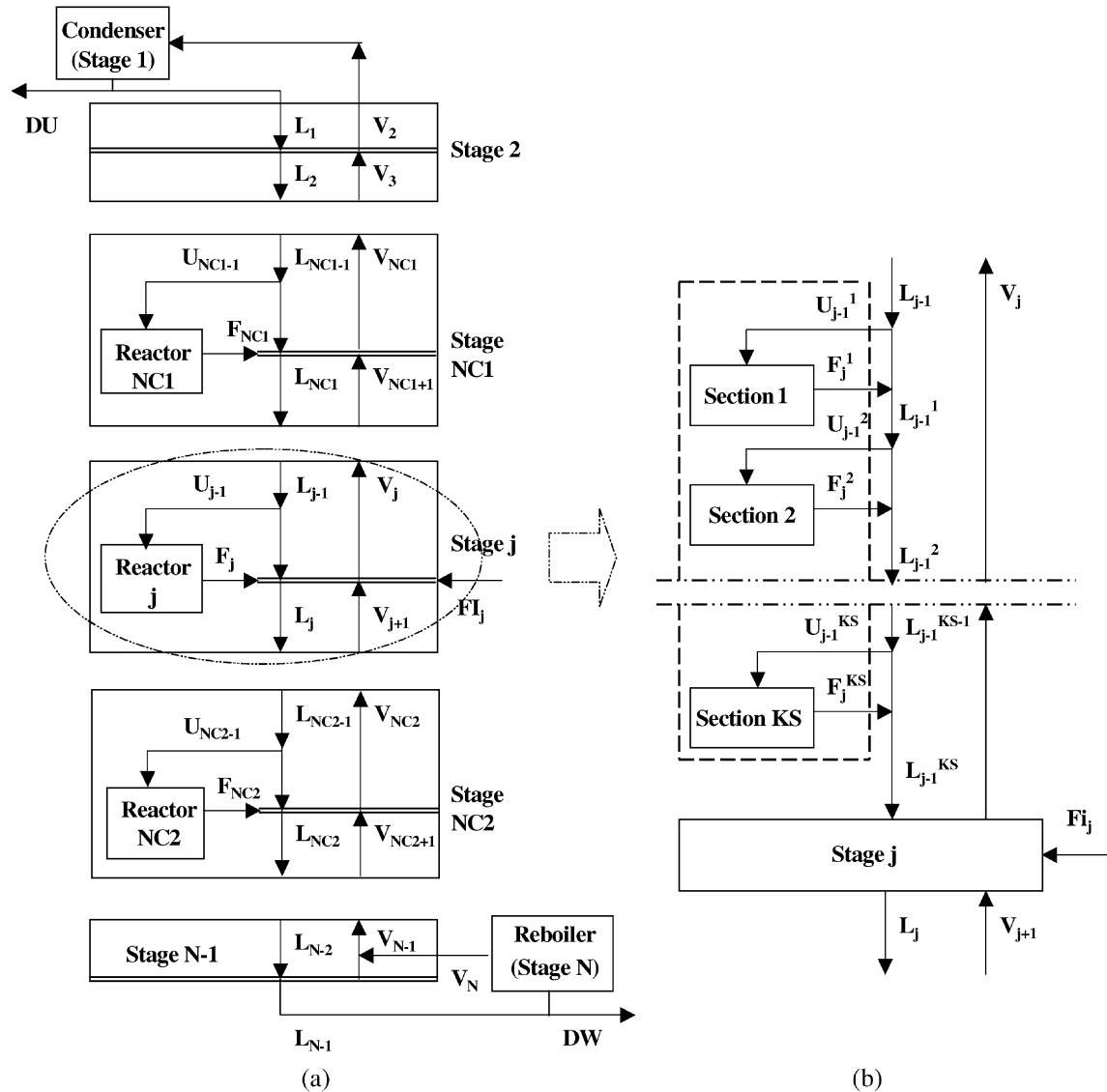
Fig. 1. Schematic diagram and configuration of catalytic-distillation column: (a) whole column model; (b) equilibrium stage model.

transfer are neglected at the equilibrium stage. The reaction is considered taking place in the liquid phase.

3.2. Model equations

The model equations based on the typical equilibrium stage j are shown as follows:

(1) Mass balance equation:

$$\frac{d(E_j x_{j,i})}{dt} = L_{j-1} x_{j-1,i} + V_{j+1,i} y_{j+1,i} - L_j x_{j,i} - V_j y_{j,i} + FI_j ZI_{j,i} + \Delta R_{j,i} \quad (7)$$

where FI_j and ZI_j are the feedstock flowrate and composition at stage j (NF1 or NF2), respectively. $\Delta R_{j,i}$ is the consumption rate for component i at stage j. The terms of $\Delta R_{j,i} > 0$, $\Delta R_{j,i} < 0$ and $\Delta R_{j,i} = 0$ correspond

to the reactants, the products, and the unreacted components, respectively.

(2) Reaction equations:

The reaction kinetics equation (2) is rearranged regarding to isobutylene conversion X_B for the merit of application convenience as shown in Eq. (8):

$$X_B = \frac{k_1}{k_1 + k_2} \left[1 - \exp\left(-(k_1 + k_2)\frac{V_C}{V_L} \right) \right]$$
$$= \frac{k_1}{k_1 + k_2} \left[1 - \exp\left(-\frac{k_1 + k_2}{V_T} \right) \right] \quad (8)$$

where V_C is the catalyst volume, V_L the liquid volumetric flowrate flowing through the catalyst and V_T ($=V_L/V_C$) is the catalyst space velocity, meaning the liquid volumetric rate flowing through per volume unit of solid catalyst. The swelling of the catalyst is taken into

account in the volume calculation (20% increase in volume after the dry resin catalyst particles are bathed in liquid). V_T is decided by the catalyst amount and the liquid flowrate of the column. The reciprocal of V_T, $1/V_T$, indicates the contacting time of liquid with catalyst, corresponding to the liquid residue time in the homogeneous reactive-distillation process. The difference between the two parameters is that the liquid residue time in the homogeneous process is a parameter used for both reaction and separation, while the space velocity V_T is only used to describe the reaction behaviors in the heterogeneous process. The liquid residue time in the heterogeneous process is also calculated at each equilibrium stage but it has no direct relations to the reaction behaviors, since the reaction and separation occurs at different locations of the catalytic-distillation column (reaction in the catalyst package, and separation in the trays or packings).

The consumption rate $\Delta R_{j,i}$ on stage j is calculated in Eq. (9). The catalyst space velocity on each catalyst package is calculated to give the conversion yield of isobutylene at each package:

$$\Delta R_{j,i} = \sum_{k=1}^{KS} \alpha L_{j-1}^k \frac{k_1}{k_1 + k_2} \times \left[1 - \exp\left(-\frac{\delta(k_1 + k_2)V_C}{(NC2 - NC1 + 1) \cdot KS \cdot \alpha L_{j-1}^k \rho_j} \right) \right] \tag{9}$$

where ρ_j is the liquid molar density, k the layer of catalyst package at stage j ($1 \leq k \leq KS$), α the contacting efficiency of liquid to catalyst, and δ is the reaction efficiency in the catalyst package. The value for α and δ in the two industrial cases was taken to be unity, because of the reasons described in Section 3.1.

(3) Vapor–liquid equilibrium equation:

$$y_{j,i} = K_{j,i} x_{j,i} \tag{10}$$

where $K_{j,i}$ is the vapor–liquid equilibrium coefficient for component i at stage j, calculated from Eqs. (5) and (6).

(4) Component summation equations:

$$\sum_{i=1}^{c} x_{j,i} = 1 \tag{11}$$

$$\sum_{i=1}^{c} y_{j,i} = 1 \tag{12}$$

(5) Enthalpy balance equations:

$$L_{j-1}h_{j-1} + V_{j+1}H_{j+1} - L_j h_j - V_j H_j + FI_j HI_j + \Delta Q_j = 0 \tag{13}$$

$$\Delta Q_j = \Delta H_j \Delta R_{j,i} \tag{14}$$

where HI_j is the molar enthalpy of feedstock, and ΔH_j and ΔQ_j are the molar heat of reaction and total heat of reaction at stage j, respectively.

The model equations (Eqs. (7)–(14)) are rearranged into the form of tridiagonal matrix as shown in Eq. (15):

$$A_j x_{j-1,i}^{t+1} + B_j x_{j,i}^{t+1} + C_j x_{j+1,i}^{t+1} = D_j \tag{15}$$

where the matrix coefficients A_j, B_j, C_j, D_j take different values at the different section of the column from $N = 1, 2$ to $NC1-1$; $NC1$, $NC1+1$ to $NC2-1$; $NC2$, $NC2+1$ to $N-1$ and N. The independent variables in the catalytic-distillation column include the number of equilibrium stages N, the number of package layers at each stage KS, the locations of the methanol and mixed C4 feedstock streams $NF1$ and $NF2$, the start and end stages of catalyst packing $NC1$ and $NC2$, the pressure on the top stage, the pressure drop of the column (or the pressure on the bottom), the catalyst volume packed in the column V_C, the reflux ratio, the reflux temperature, distillate flowrate, and the feedstock flowrate and composition variables. The model equations (Eqs. (7)–(14)) are simultaneously solved using the relaxation algorithm after the independent variables, and the relaxation coefficient and the initial values of the parameters are given. The diagram of the detailed calculation flowsheet is shown in Fig. 2.

3.3. Design of catalytic-distillation user modular on Aspen plus platform

(1) The program is written into the user modular using the built-in Fortran language following the grammar and communication rules issued by Aspen plus system, and then compiled it into an executive file using NDP Fortran compiler.

(2) The reaction kinetic model is developed as a subroutine of the user modular.

(3) The vapor–liquid equilibrium model is developed by calling NRTL equation for liquid activity coefficient calculations and Redlick–Kwong–Soave equation for vapor fugacity calculations. The NRTL binary interaction parameters b_{ij}, b_{ji} and α_{ij} estimated from the experimental data are applied to replace the data from UNIFAC model in Aspen plus.

(4) Other general thermodynamic properties are calculated by calling DIPPR database through the subroutines such as VTHRM for vapor pure substance properties, LTHRM for liquid pure substance properties, VMTHMY for vapor mixture properties, LMTHMY for liquid mixture properties, ENTHV for vapor mixture enthalpy, ENTHL for liquid mixture enthalpy, VOLV for vapor mixture molar volume, VOLL for liquid mixture molar volume, FUGV for vapor mixture fugacity, FUGLY for liquid mixture fugacity, etc.
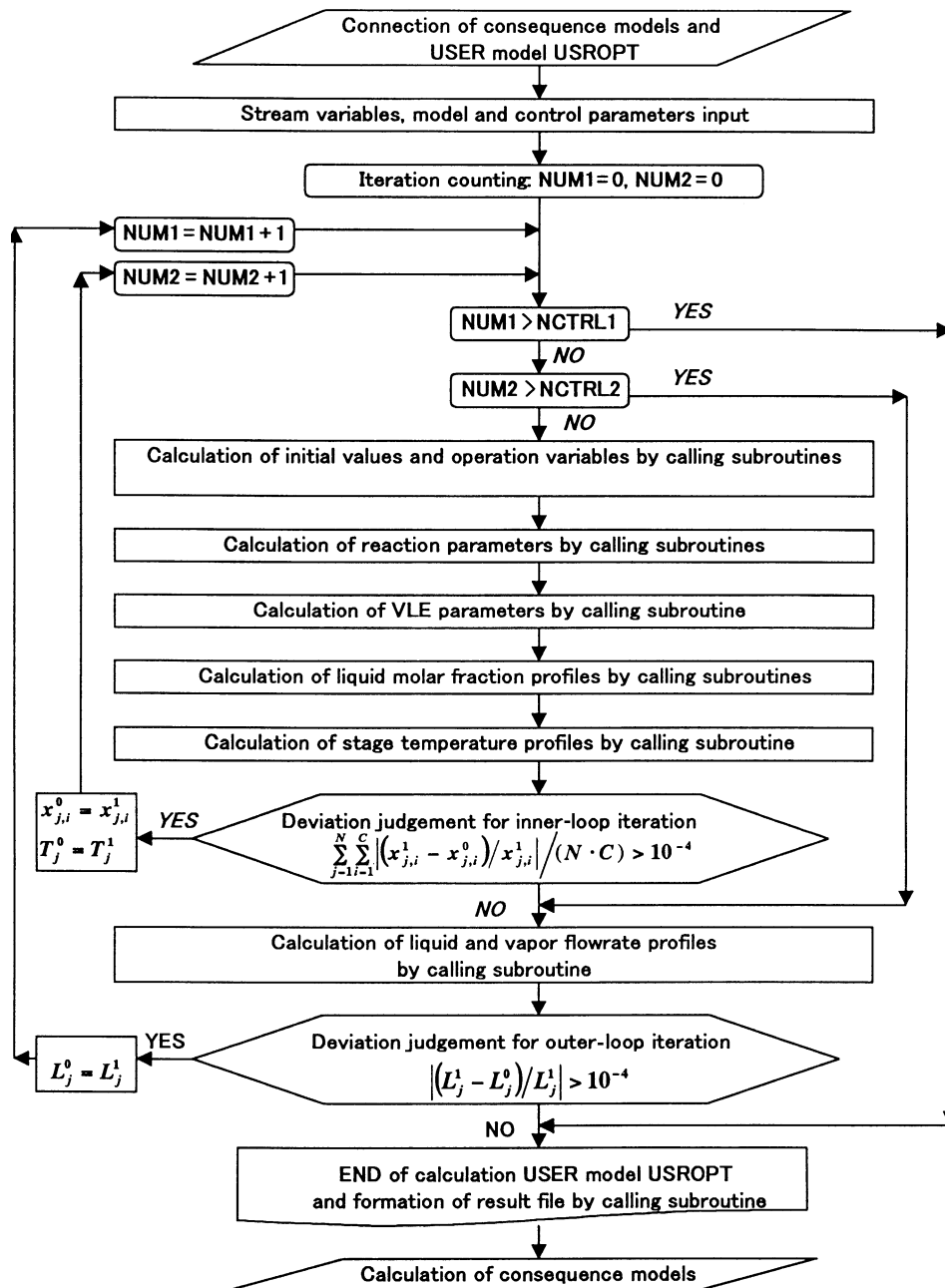
Fig. 2. Calculation flowsheet of user model USROPT developed for simulating catalytic-distillation column.

(5) The communication between the user modular and other system modules, database, function tools and monitor systems are realized through the connection of material streams, enthalpy and entropy streams as well as information streams according to the rules and formats of Aspen plus system.

(6) Writing the input parameters, calculation results and calculation information into the report files by calling common subroutines.

The detailed communication and calling processes are also shown in Fig. 2. The user program USROPT includes one main program and 13 self-defined subroutines.

4. Results and discussion

4.1. Simulation of Plant A using loose-stack package technology

Fig. 3(a) shows the industrial flowsheet of Plant A using the loose-stack package technology in the catalytic-distillation column with the annual MTBE production of 20,000 t. The mixed C4 hydrocarbons containing about 32% (wt.) isobutylene is mixed with methanol in the static mixer V-2 and then pumped into the pre-reactor R-1, in which about 90% isobutylene is converted. The products
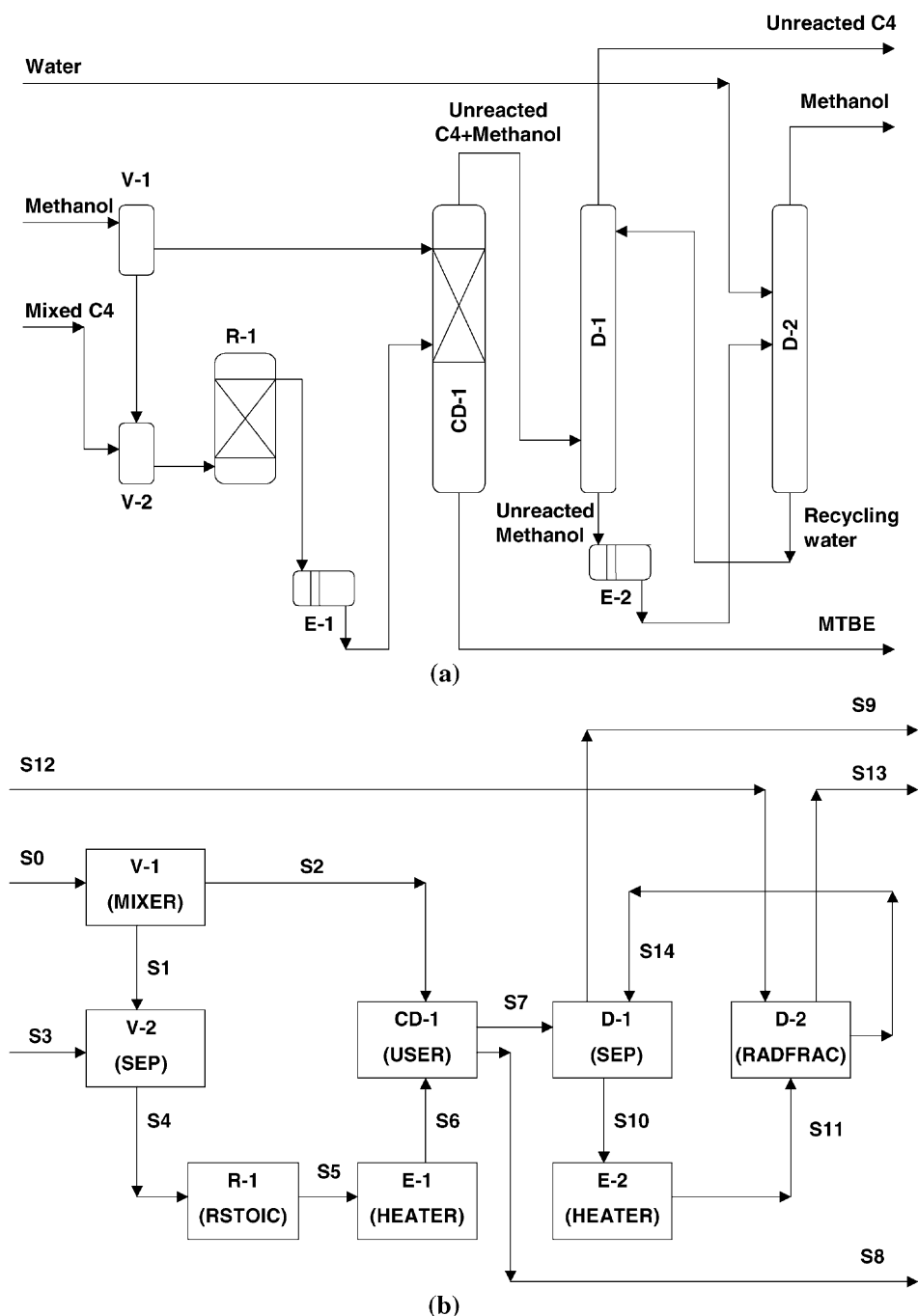
Fig. 3. Diagrams of (a) industrial and (b) Aspen plus flowsheets of Plant A.

from R-1 are fed into the catalytic-distillation column CD-1 after the heat exchanger E-1. The methanol feedstock is split into two streams by the splitter V-1; one is mixed with the mixed C4 in the static mixer V-2 as described above, the other is fed into CD-1 directly at the upper location of the column. The sulphonic ion-exchange resin catalysts packing in the loose-stack envelopes are installed in the reactive section of CD-1. The MTBE product is obtained as the bottom products of CD-1. The distillate containing the unreacted C4 hydrocarbons and methanol are fed into the water stripper column D-1. The hydrocarbons are recovered from the top of D-1, and the methanol/water mixture from the bottom of D-1 is fed into the methanol distillation column D-2 after another heat exchanger E-2. The methanol is recovered as the distillate of D-2 (the recycling of methanol is not included in the flowsheet). Water from the bottom of D-2 is also fed back to D-1 for recycling. Fresh water is added to D-2 to compensate the loss in D-1 and D-2.

The Aspen plus flowsheet of Plant A is shown in Fig. 3(b). The splitter V-1 and static mixer V-2 are represented by MIXER modules, the pre-reactor R-1 by RSTOIC modular, the heat exchangers E-1 and E-2 by HEATER modules, the catalytic-distillation column CD-1 by USER modular USROPT, the water stripper D-1 by SEP modular, and the methanol distillation column D-2 by RADFRAC modular. The NRTL equation and Redlick–Kwong–Soave equation are applied for the whole flowsheet except the water stripper D-1. In D-1, the UNIF-LL equation is applied because of the existence of the liquid–liquid equilibrium inside D-1. There are 14 streams, 8 unit operation blocks, 1 tear stream and 1 design-spec block included in the Aspen plus flowsheet.

The catalytic-distillation column CD-1 is the key equipment of the Plant A. The rectification section is packed with structured packings, with 4 m in height and 1 m in diameter. The reactive section is packed with 10 layers of the catalyst packages and 10 layers of the valve trays, with 23 m in height and 1.4 m in diameter. The stripping section is packed with 30 layers of the valve trays, with 14.5 m in height and 1.4 m in diameter. Before the catalytic-distillation technology was put into application, MTBE was commercially produced in the fixed-bed reactor using the same catalysts [3]. The separation of the MTBE products was carried out in a distillation column using the same kind of the valve trays and structured packings. The efficiency of the valve trays and the HETP height of the structured packings were determined in the rating experiments of the industrial distillation column. The efficiency or HETP data obtained were used to calculate the number of the equilibrium stages in the current industrial catalytic-distillation column. The data are shown in Table 3.

Three operating cases with different flowrates of the mixed C4 and methanol were simulated as shown in Table 3. The conversion yields of isobutylene in R-1 were 91.81, 92.52 and 92.76% in Cases 1–3, respectively. Table 3 shows that the calculated compositions in both distillate and bottom streams of CD-1 agree well with the operating data. The calculated isobutylene conversion in each case is also close to the operating data. The axial distributions of isobutylene, methanol, MTBE, and temperature profiles are shown in Fig. 4. The figure indicates that the calculated temperature profiles are in good agreements with the operating data. It can be concluded that the user modular can be used in the flowsheet simulation of the catalytic-distillation process with the loose-stack-type catalyst package.

The kinetic study shows that the molar ratio of methanol to isobutylene should be no less than 0.8 to prevent the dimerization of isobutylene. The molar ratios of methanol to isobutylene in the feedstock to CD-1 are 1.58, 2.54 and 2.36 for Cases 1–3, respectively. Fig. 4(a) shows an axial distribution of low methanol concentration, particularly in the reactive section. This fact indicates that Case 1 might be under the risk of isobutylene dimerization due to the deficiency of methanol in the feedstock. On the other hand, Case 2 gives

Table 3
Comparison between calculated and operating results in Plant A

Operating conditions	Case 1		Case 2		Case 3	
Number of equilibrium stage (excluding condenser and reboiler)	32		32		32	
Rectification section	7		7		7	
Reactive section	10		10		10	
Stripping section	15		15		15	
Mixed C4/methanol feedstock (kg/h)	8090		9860		8170	
Methanol feedstock (kg/h)	130		150		130	
Feedstock temperature (°C)	66.7		68.6		77.2	
Isobutylene in feedstock (wt.%)	2.45		2.45		2.32	
Methanol in feedstock (wt.%)	0.61		2.03		1.54	
Catalyst weight (kg)	3500		3500		3500	
Reflux flowrate (kg/h)	4680		5920		5021	
Reflux temperature (°C)	46.0		76.4		56.9	
Pressure at top (MPa)	0.80		0.80		0.80	
Pressure at bottom (MPa)	0.85		0.85		0.85	

| Results	Case 1		Case 2		Case 3	
	Operating data	Calculated data	Operating data	Calculated data	Operating data	Calculated data
Composition (wt.%)						
Isobutylene in distillate	0.06	0.048	0.07	0.054	0.08	0.037
MTBE in bottom	99.54	99.68	99.36	99.62	99.33	99.45
TBA in bottom	0.79	0.048	0.41	0.082	0.42	0.06
Methanol in bottom	0.05	0.25	0.06	0.24	0.05	0.36
C4 in bottom	0.11	0.07	0.17	0.06	0.09	0.13
Conversion yield of isobutylene (%)						
CD-1	98.17	98.86	98.04	99.70	97.66	99.08
Total process	99.85	99.90	99.83	99.88	99.83	99.92
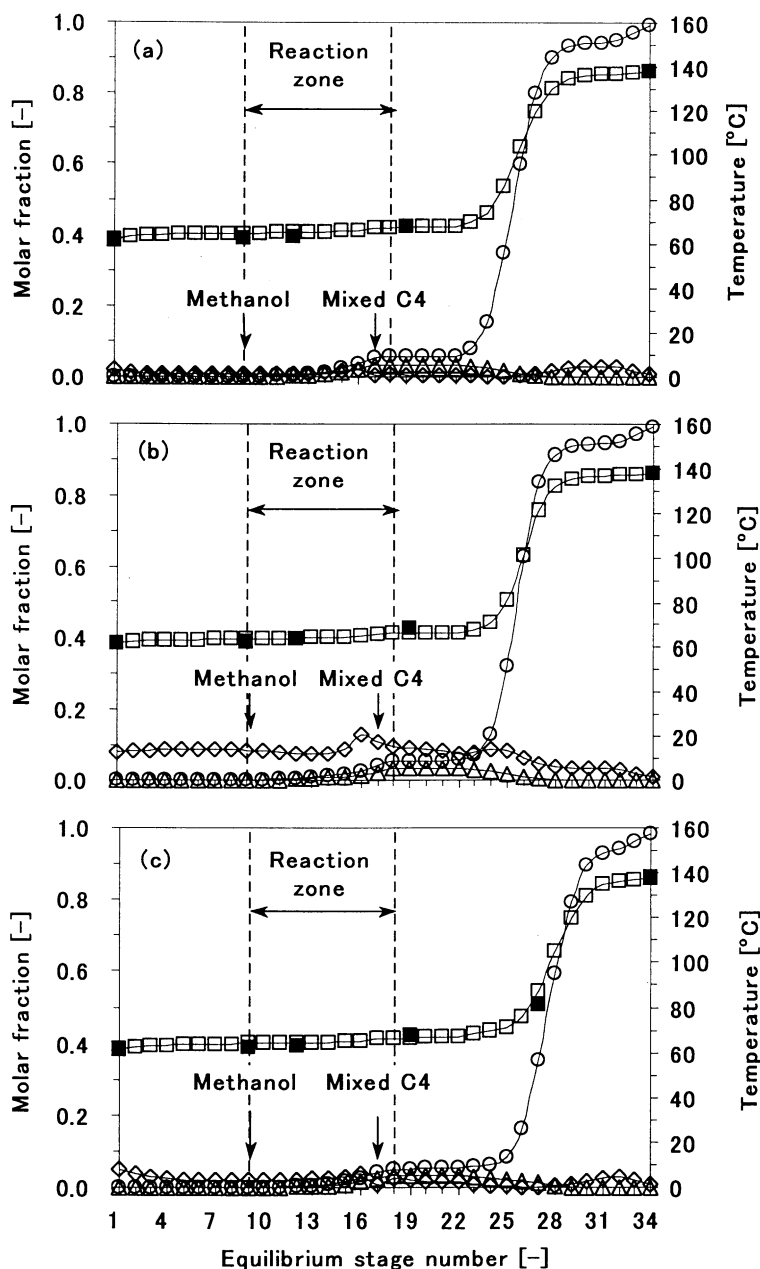
Fig. 4. Axial distributions of component concentrations and temperature along column height for Plant A ((a) Case 1; (b) Case 2; (c) Case 3): (○, △, ◇) calculated molar fractions of MTBE, isobutylene and methanol, respectively; (□, ■) calculated and observed stage temperatures, respectively.

an opposite tendency of the axial methanol distribution as shown in Fig. 4(b), in which the axial ratio of methanol to isobutylene is too high due to the higher methanol feedstock. This leads to a high methanol concentration in the distillate, and consequently, the high methanol concentration in the distillate increases the operating cost of the water stripper D-1 and methanol distillation column D-2. Case 3 gives a reasonable axial methanol distribution as shown in Fig. 4(c), indicating that the optimal molar ratio of methanol to isobutylene in the feedstock might be around 2.36.

It is also found from Fig. 4 that the peak value of the isobutylene and methanol concentrations appears in the

stripping section. This might indicate that the present feedstock location at stage 17 is too low to take advantage of higher reactant concentrations as the driving forces of reaction.

4.2. Simulation of Plant B using bale-type package technology

Another industrial application is for Plant B using the bale-type package technology in the catalytic-distillation column with the MTBE production of 40,000 t annually as shown in Fig. 5(a). The catalytic-distillation column DA-301
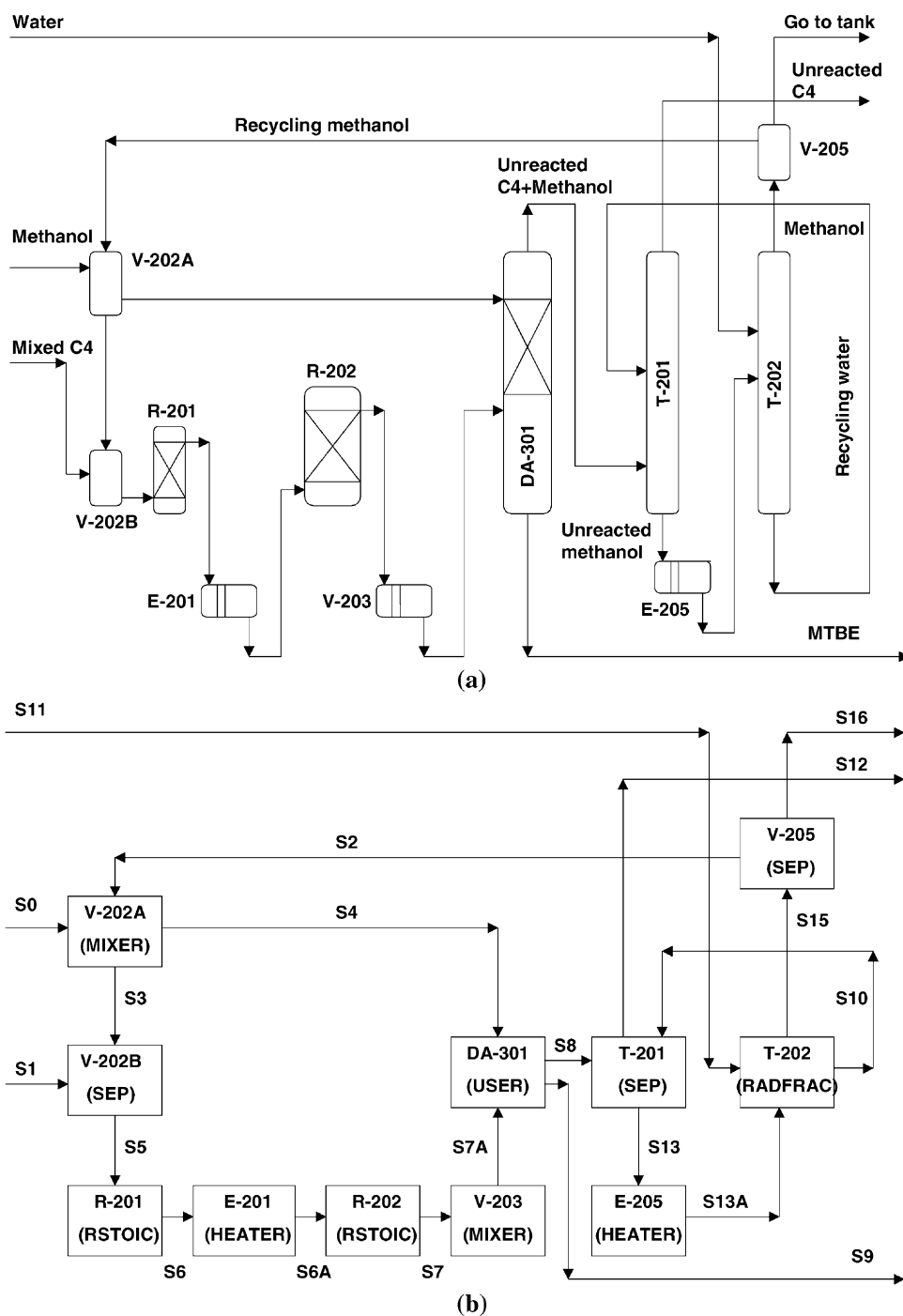
Fig. 5. Diagrams of (a) industrial and (b) Aspen plus flowsheets of Plant B.

is composed of two columns, the combination of the rectification and reactive sections as the upper column, with 36 m in height and 0.95 m in diameter, and the stripping section as the down column. The upper column is 56 m in height and 2.2 m in diameter. The down column is 15 m in height and 1.05 m in diameter. The rectification section is packed with 10 layers of the valve trays. The reactive section is packed with 9 layers of the catalyst packages. The stripping section

is packed with 25 layers of the valve trays. The numbers of the equilibrium stages in each section of the column DA-301 were obtained in the industrial rating tests, carried out soon after Plant B was operated to its optimal conditions. The data obtained are shown in Table 4.

Plant B is more complicated than Plant A because the methanol recycling is taken into account. The mixed C4 hydrocarbons containing about 40 wt.% isobutylene is mixed

Table 4
Comparison between calculated and operating results in Plant B

Operation conditions	Value			
Number of equilibrium stage (excluding condenser and reboiler)	29			
Rectification section	7			
Reactive section	9			
Stripping section	13			
Mixed C4/methanol feedstock to DA-301 (kg/h)	10596			
Methanol feedstock to DA-301 (kg/h)	280			
Feedstock temperature to DA-301 (°C)	60.0			
Isobutylene concentration to DA-301 (wt.%)	3.23			
Methanol concentration to DA-301 (wt.%)	2.29			
Catalyst weight in DA-301 (kg)	1473			
Reflux flowrate in DA-301 (kg/h)	2759.4			
Reflux temperature in DA-301 (°C)	40.0			
Pressure at top of DA-301 (MPa)	0.784			
Pressure at bottom of DA-301 (MPa)	0.945			
Results	Distillate		Bottom stream	
	Operating data	Calculated data	Operating data	Calculated data
Compositions (wt.%)				
Propylene	1.14	1.13	0.00	0.00
Isobutene	1.03	1.03	0.00	0.00
1-Butane	3.11	3.09	0.02	0.00
1-Butylene	57.13	56.72	0.09	0.00
Isobutylene	0.24	0.44	0.00	0.00
Trans-2-butylene	20.34	20.37	0.17	0.00
Cis-2-butylene	12.38	12.50	0.19	0.00
Methanol	4.61	4.71	0.02	0.80
Methyl tert-butyl ether	0.00	0.00	98.64	98.66
Diisobutylene	0.00	0.00	0.68	0.43
Tert-butyl alcohol	0.00	0.00	0.19	0.10
Water	0.00	0.00	0.00	0.01
Operating parameters	Operating data		Calculated data	
Distillate flowrate (kg/h)	5494.00		5494.00	
Bottom flowrate (kg/h)	5428.43		5428.43	
Distillate temperature (°C)	63.00		62.00	
Bottom temperature (°C)	144		142.39	
Isobutylene conversion (%)	96.30		92.96	
Total isobutylene conversion (%)	99.62		99.30	

with methanol in static mixer V-202B and then pumped into the protective reactor R-201 to remove the harmful heavy metal ions. The stream enters the pre-reactor R-202 consequently after a heat exchanger E-201 in which about 90% isobutylene is converted. The product stream from R-202 is fed into the main catalytic-distillation column DA-301 after another heat exchanger V-203. The methanol feedstock is split into two streams by the splitter V-202A; one is mixed with the mixed C4 in the static mixer V-202B as described above, and the other is fed into DA-301 directly. The catalyst particles packed into the bale-type envelopes are installed in the middle section of DA-301. MTBE is obtained as the bottom products of DA-301. The unreacted C4 hydrocarbons and methanol from the distillate of DA-301 are fed into the water stripper column T-201. The hydrocarbons are recovered from the top stream of T-201. The methanol/water mixture from the bottom of T-201 after a heat exchanger E-205 is fed into the methanol distillation column T-202 for

the recovery of methanol. The unreacted methanol is recovered as the distillate and recycled back to V-202A as the methanol feedstock again. Part of the recovered methanol is removed to tank reservoir in the splitter V-205. Water is recovered as the bottom stream of T-202, and then fed back to T-201. Fresh water is added to T-202 to compensate the loss in T-201 and T-202.

The Aspen plus flowsheet for Plant B is shown in Fig. 5(b). The splitter V-202A is represented by MIXER modular, the static mixer V-202B, the splitter V-205 and water stripper T-201 by SEP modules, the protective reactor R-201 and main reactor R-202 by RSTOIC modules, the heat exchangers E-201 and E-205 by HEATER modules, the heat exchanger V-203 by MIXER modular, the catalytic-distillation column DA-301 by USER modular USROPT, and the methanol distillation column T-202 by RADFRAC modular. Similar to the simulation of Plant A, the modified NRTL equation and Redlick–Kwong–Soave
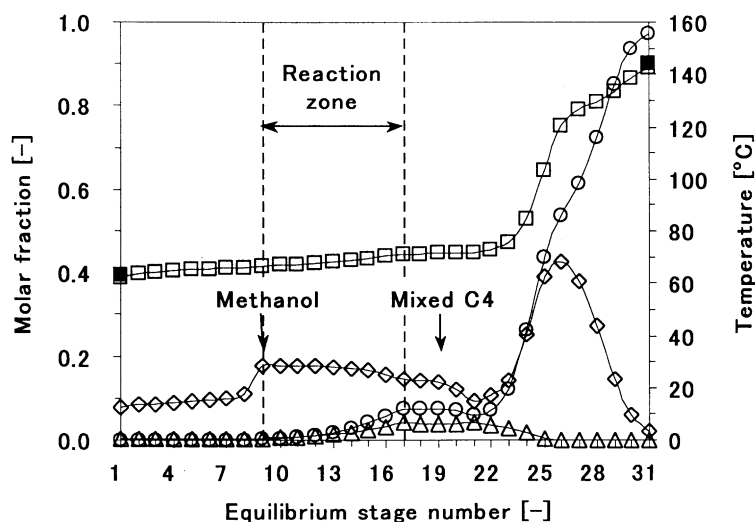
Fig. 6. Axial distribution of component concentrations and temperature along column height for Plant B: ($\bigcirc$, $\triangle$, $\diamond$) calculated molar fractions of MTBE, isobutylene and methanol, respectively; ($\square$, $\blacksquare$) calculated and observed stage temperatures, respectively.

equation of state are applied in the whole flowsheet except D-1 in which the UNIF-LL equation is applied. There are 11 unit operation blocks, 19 streams, 2 tear streams, 1 design-spec block, 2 convergence blocks and 1 on-line Fortran block in the Aspen plus flowsheet as shown in Fig. 5(b).

Table 4 shows that the calculated component concentrations in both distillate and bottom stream of DA-301 agree well with the operating data. The axial distributions of isobutylene, methanol, MTBE, and temperature profiles are shown in Fig. 6. The calculated temperature profiles are in good agreement with the operating data. It indicates that the user modular can be used in the flowsheet simulation of catalytic-distillation process with the bale-type catalyst package.

The calculated conversion of isobutylene is 3.34% lower than the observed one although the total conversion of isobutylene is very close. A possible explanation is given. In the real operation, a small portion of catalyst particles was gradually ground into powder in the strikes with the upward vapor streams and downward liquid streams in the long-term operation. The powders slowly moved out of the catalyst bales and settled down in the bottom reboiler. The accumulation of the catalyst powders in the reboiler caused MTBE to decompose, and let the MTBE concentration below the product standard 98 wt.% with higher methanol concentration in the product. Therefore, the catalyst powders had to be removed from the reboiler during the periodic maintenance of the equipment. However, the catalyst amount used in the calculation was measured after 2 years' operation in the maintenance. Obviously, the real catalyst amount should be larger than the measured data, because the catalyst loss could not be included. This loss of catalyst might be responsible for the isobutylene conversion decrease. Different from Plant B, Plant A was a new equipment. The catalyst weight was measured

before the operation started. The operating data were also obtained several days after the start-up of the plant. So there is no significant difference in the conversion yield of isobutylene between the calculated and operating data for Plant A.

The molar ratio of methanol to isobutylene in the feedstock to DA-301 is 2.67. This ratio is even much higher than that of Plant A in Case 2. So it is not surprising to find that the axial methanol concentration shows an unreasonable distribution. A big peak of the methanol concentration is found near the bottom besides the one in the reactive section. To improve the present situation, the following measures should be taken: (1) to increase the feeding location of mixed C4 stream; (2) to decrease methanol in the feedstock to the ratio of methanol to isobutylene of 2.36.

5. Conclusion

(1) The industrial catalytic-distillation process for the MTBE production was simulated by developing the catalytic-distillation model as a user modular on the Aspen plus platform, taking advantage of the strong database, flexible simulation functions and optimization tools of the Aspen plus system, while retaining the characteristics of the previous verified model.

(2) The experimentally determined reaction kinetics was applied in the model. NRTL and Redlick–Kwong–Soave equations were selected for the vapor–liquid equilibrium calculation. The NRTL binary interaction parameters were estimated from the experimental data of the two-component vapor–liquid equilibrium.

(3) The flowsheet simulations of the two industrial plants, using the loose-stack-type package and the bale-type

package technologies in the catalytic-distillation column, were simulated on the Aspen plus platform. The results show that fair agreements between the calculated and operating data were obtained.

References

[1] M.M. Sharma, Separation through reaction, J. Sep. Process Technol. 6 (1985) 9–16.

[2] M.F. Doherty, G. Buzad, Reactive distillation by design, Chem. Eng. Res. Design, Trans. Inst. Chem. Eng. (Part A) 70 (1992) 448–458.

[3] X. Hao, J. Wang, Z. Yang, J. Bao, Novel catafractionation technology for the production of methyl *tert*-butyl ether, Chem. Eng. J. 56 (1995) 11–18.

[4] J.G. Stichlmair, T. Frey, Reactive distillation processes, Chem. Eng. Technol. 22 (1999) 95–103.

[5] R. Taylor, R. Krishna, Modeling reactive distillation, Chem. Eng. Sci. 55 (2000) 5183–5229.

[6] J. Bao, G. Yan, X. Wu, Mathematical simulation of the non-homogeneous catalytic-distillation process for MTBE production, Chem. Eng. (China) 22 (5) (1994) 6–12.

[7] S. Venkataraman, W.K. Chen, J.F. Boston, Reactive distillation using Aspen plus, Chem. Eng. Prog. 86 (1990) 45–54.

[8] AspenTech User Guide Reference for Aspen Plus System, Vols. 1–6, 1994.

[9] Z. Yang, M. Liu, X. Luan, Macroscopic kinetics for MTBE synthesis using macroporous ion-exchange resin catalyst, Qilu Petrochem. Technol. (China) 12 (1) (1984) 27–31.

[10] M.J. Lockett, Distillation Tray Fundamentals, Cambridge University Press, Cambridge, UK, 1986.

[11] J.G. Stichlmair, J.R. Fair, Distillation Principal and Practice, Wiley, New York, 1999.

[12] G.P. Towler, S.J. Frey, Reactive distillation, in: S. Kulprathipanja (Ed.), Reactive Separation Process, Taylor & Francis, Philadelphia, 2000.

[13] K.H. Johnson, A.B. Dallas, Catalytic distillation structure, US Patent 5 336 373 (1993).

[14] L.A. Smith Jr., Catalytic distillation structure, US Patent 4 443 599 (1984).

[15] L.A. Smith Jr., Catalytic distillation process and catalyst, European Patent 008860B1 (1985).

[16] C.S. Crossland, G.R. Gildert, D. Hearn, Catalytic distillation structure, US Patent 5 431 890 (1995).

[17] Chinese Patent ZL 90 1 095265.5; ZL 88 1 09705.5.